Journal of Plankton Research Vol.21 no.3 pp.445–464, 1999

Stable model structures for representing biogeochemical diversity and size spectra in plankton communities

Robert A.Armstrong

Program in Atmospheric and Oceanic Sciences, Sayre Hall, PO Box CN710, Princeton University, Princeton, NJ 08544-0710, USA

Abstract. There is a fundamental duality in the way we view planktonic communities. On one hand, we see these communities as composed of a diverse mixture of taxonomically and biogeochemically distinct species; pelagic ecosystem models capable of predicting the ocean's role in the global carbon cycle will need to resolve these multiple plankton taxa. However, we have also come to appreciate that superimposed on this diversity are regular patterns of size structure, where plots of abundance within size classes typically show a power-law dependence on size. A truly complete model description of planktonic community structure must reflect both aspects of this duality. Here I examine two classes of ecosystem models that are capable of representing this duality. The first structure is based on multiple (n) couplets of phytoplankton (P) and zooplankton (Z) [an '$n(PZ)$' model]. Within certain regions of parameter space, this model structure can produce anomalous oscillatory behaviors, the mathematical origin of which is explored in detail. I then examine an alternative food web structure in which total herbivore abundance is represented by a single state variable, G, and where grazing pressure is distributed among taxa in proportion to their abundances. This '$(nP)G$' system is stabilized by the redistribution of grazing intensity among taxa in response to changes in their densities. This 'distributed grazing' model also naturally produces size spectra of plankton abundance; this last observation argues that the model with distributed grazing can help in uncovering and representing the mechanistic basis for the genesis and maintenance of planktonic size spectra of phytoplankton and bacteria.

Introduction

In pelagic ecosystem models used for ocean biogeochemistry, it will often be necessary to include a variety of biological taxa whose presences have different geochemical implications (Totterdell *et al*., 1994). For example, in studies of the ocean's role in the global carbon cycle, the relative proportions of diatoms and coccolithophorids in the phytoplankton are of obvious importance, since conditions favoring coccolithophorids over diatoms lead to enhanced precipitation of calcium carbonate, which in turn lowers alkalinity and increases the partial pressure of carbon dioxide (Broecker and Peng, 1982). Similarly, nitrogen fixers will need to be included, since their activity can increase new production, increasing the potential for oceanic uptake of carbon dioxide from the atmosphere (Capone *et al*., 1997; Falkowski, 1997), and because they may also determine whether a given region of the ocean is limited by nitrogen or by phosphate (Karl *et al*., 1997). Finally, different algal size classes and taxa may be grazed by predators whose fecal pellets sink at different speeds, which may in turn influence the depth at which remineralization occurs (Totterdell *et al*., 1994).

A fundamental question then arises: given the necessity of including diverse taxonomic groups, how is this goal most naturally attained? One way to proceed is first to recognize that there is a fundamental duality in the way we view planktonic communities. On one hand, we see these communities as composed of a diverse mixture of taxonomically and biogeochemically distinct species. But we

© Oxford University Press

have also come to appreciate that superimposed on this diversity are regular patterns of size structure, where plots of abundance within size classes typically show a power-law dependence on size (Sheldon *et al.*, 1972; Sprules, 1988; Chisholm, 1992; Gin, 1996; Vidondo *et al.*, 1997). Any putatively complete model description of plankton community structure must reflect both aspects of this duality.

As a first attempt at producing a model that could reflect both parts of this duality, Armstrong (1994) proposed a model with n parallel food chains, each consisting of a phytoplankton species P_i and its dedicated zooplankton predator Z_i (Figure 1a). Each phytoplankton–zooplankton couplet was taken to represent a different size class. Parameter values for successive size classes were taken to vary allometrically (i.e. as a power law) with size (Moloney and Field, 1989, 1991), with smaller size classes growing more rapidly and being consumed more rapidly by their zooplankton predators. In this model, as total nutrient in the system is increased, phytoplankton–zooplankton pairs are added sequentially, starting with the smallest size classes, which are competitively favored because of their large surface-to-volume ratios. As total nutrient is increased from very low levels, the smallest autotrophic size class P_1 invades the system, followed by its specialized grazer Z_1. As more nutrient is added, species and size classes are added in the sequence P_i, Z_i, P_{i+1}, and so forth, where size increases with i. The pattern produced by this sequence is one of 'equal biomass in equal logarithmic size categories' (Chisholm, 1992), where total phytoplankton biomass increases by the addition of larger size classes rather than through increases in existing size classes [Raimbault *et al.*, 1988; Chisholm, 1992; see also Figure 2 of Armstrong (1994)].

This simple model of parallel food chains was later found to have several undesirable properties when used to model time series data (G.C.Hurtt and R.A.Armstrong, personal observation). First, as total nutrient loading is increased, prey species P_i will invade the system without its specialized grazer Z_i. While this does not hinder the model's effectiveness at describing steady-state conditions (Armstrong, 1994), it does cause problems with fitting non-steady-state data, because the ungrazed largest size class can take up large amounts of

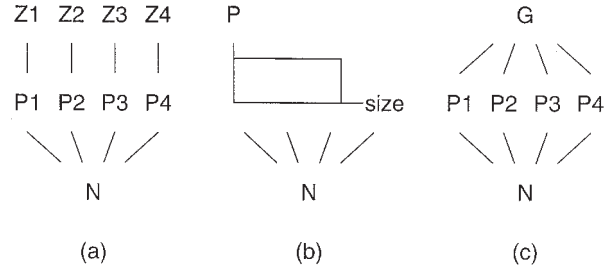

Fig. 1. Three models with multiple phytoplankton species: (**a**) multiple parallel food chains; (**b**) parameterized size dependence with constant biomass density in size classes for sizes below some maximum size; (**c**) distributed grazing.

limiting nutrient during blooms, which (being ungrazed) it only slowly returns to the system during the rest of the year.

The model can be generalized to overcome this problem by allowing zooplankton size class *i* also to prey on smaller zooplankton size classes and on additional phytoplankton size classes (Moloney and Field, 1991; Moloney *et al*., 1991; Armstrong, 1994; Armstrong *et al*., 1994): with added food web complexity, grazer Z_i is supported by additional food sources, and so will tend already to be present when phytoplankter P_i invades [see, for example, Figure 3 of Armstrong (1994)]. However, as this figure also shows, this fix for one problem gives rise to a different problem: the set of species that will be present at a given nutrient loading now becomes extremely sensitive to choices of parameter values and food web structure (see also Armstrong *et al*., 1994).

Finally, models with these structures are often dynamically unstable in ways that are biologically unrealistic. For example, the multiple-size-class simulations of Moloney *et al*. (1991) show striking oscillations in phytoplankton and zooplankton densities. In their simulation of the Benguela upwelling (their Figures 8 and 9), densities of 'picophytoplankton' (0.2–1 μm) show regular spikes in abundance, going from virtually zero to ~400 mg C m^{-3} in each spike, with a period of ~2 days, while the 'phytoflagellates' (1–5 μm) show similar spikes at an interval of ~7 days; corresponding classes of zooplankton show similar oscillations. Their simulation of the Agulhas Bank (their Figures 4 and 5) is even more unstable, with picophytoplankton densities spiking irregularly (perhaps chaotically) at intervals of less than a day. Their 'oceanic' simulation is considerably more stable, but the smallest zooplankton size class still shows sawtooth changes in densities of a factor of two at intervals of less than a day. Such instabilities are obviously unrealistic; they also make calibrating these models with time series data such as those from the Bermuda Atlantic Time Series study (BATS), which has a time resolution of 2–4 weeks, virtually impossible (G.C.Hurtt and R.A.Armstrong, personal observation).

In response to these problems, Hurtt and Armstrong (1996, 1999) assumed a pattern of equal biomass in equal logarithmic size classes (Figure 1b). Their model predicts how total biomass and size structure should vary in time and space, but does not address biogeochemical diversity. One way to introduce biogeochemical diversity into such a model would be to partition values of total planktonic biomass and productivity among taxa using observed patterns (e.g. diatom versus carbonate productivity; Maier-Reimer, 1993). This approach should work well where such relationships are relatively constant in time and space. In general, however, the partition fractions will themselves be dynamical variables in space, time, depth and trophic status (Letelier *et al*., 1993), suggesting that a description of multiple taxa based on competition for nutrients and differential susceptibility to herbivory will provide a more general and more fundamental approach to this problem (Armstrong, 1979, 1994; Evans, 1988; Taylor and Joint, 1990; Thingstad and Sakshaug, 1990; Lehman, 1991; Moloney and Field, 1991; Moloney *et al*., 1991; Ducklow and Fasham, 1992; Bissett *et al*., 1994).

A third approach, which overcomes the problems noted above, is to adopt a model of distributed grazing (Figure 1c). This model has the simplicity and the predictable behavior of the simple model of parallel food chains, particularly in its ability to produce particle size spectra (see the section 'Using the model of distributed grazing to produce plankton size spectra'), while still ensuring that all species present are subject to grazing [see equation (24)]. The model is also dynamically stable under a wide range of conditions (see the section 'A model of distributed grazing'). This model is similar to, but not identical with, the switching grazer model of Fasham *et al.* (1990). In particular, size-specific and taxon-specific grazing is modeled as a community-level phenomenon arising from a set of population-level interactions that is inherently too complicated to model, rather than as the switching among prey types of a single zooplankton species (Fasham *et al.*, 1990).

Here I contrast the stability properties of food web models based on parallel phytoplankton–zooplankton couplets to the stability of food webs based on distributed grazing. These analyses are based on 'symmetric' food web models (Armstrong, 1982, 1983), where the 'symmetry' arises from constraining their component parts at each trophic level to have the same mathematical form and parameter values. Because of the symmetry property, I have been able to characterize the stability (tendency to return to steady state) of these food webs when only the signs (and not the magnitudes) of certain partial derivatives are known.

I start with a simple model with n parallel food chains (the 'Janzen' model of Armstrong, 1983), where each chain contains one phytoplankton and one zooplankton taxon or size class (Figure 1a). Local stability analysis shows that the dynamical instabilities in this system arise from the transfer of stabilizing tendencies from some oscillatory modes to others; this transfer process is a generic part of the model structure (see the Appendix).

I then explore a generalization of the multiple-prey single-grazer model used by Fasham *et al.* (1990), in which a single state variable represents total grazer density, and where potential grazing is distributed among phytoplankton taxa in proportion to their abundances (Figure 1c). The redistribution of grazing pressure is assumed to operate with a characteristic time lag, allowing taxa that are currently in lower abundance (and whose grazers are presumably also less abundant) to bloom while taxa that are currently numerically dominant are not blooming. Analysis of the symmetric case shows that the redistribution of grazing pressure among phytoplankton taxa counteracts the tendency of the system to oscillate by increasing the loss rates of taxa that are temporarily more abundant; this stabilizing tendency is not lost even when there is a delay in the redistribution process, so long as this delay is not too long. Under simple assumptions relating phytoplankton growth rates to size, the model produces reasonable phytoplankton size spectra, while allowing the explicit representation of biogeochemical diversity. This formulation is also remarkably flexible, and should provide a framework for modeling a wide range of marine ecosystems.

A model with parallel food chains

Consider first a model with n parallel food chains, where food chain i is composed of both a phytoplankton taxon or size class P_i and a zooplankton taxon or size class Z_i that feeds exclusively on P_i, and where all P_i compete for some limiting nutrient N. This model (Figure 1a) may be written:

$$\begin{aligned}\frac{dP_i}{dt} &= f_{Pi}(P_i, Z_i) \\ &= P_i\,[\mu_i(N) - Z_i\,h_i(P_i)]\end{aligned} \tag{1a}$$

$$\begin{aligned}\frac{dZ_i}{dt} &= f_{Zi}(P_i, Z_i) \\ &= Z_i[\gamma_i\,P_i\,h_i(P_i) - \varepsilon_i(\sum_{j=1}^{n} Z_j)]\end{aligned} \tag{1b}$$

for $i = 1, \ldots, n$, and

$$N = T - \sum_{i=1}^{n} P_i - \sum_{i=1}^{n} Z_i \tag{1c}$$

Here $\mu_i(N)$ is the growth rate of P_i as a function of nutrient concentration N. The function $h_i(P_i)$ is the per-phytoplankton-per-zooplankton harvest rate of P_i by Z_i, so that the product $P_i h_i(P_i)$ is the per-zooplankton harvest rate (the 'functional response' sensu Holling, 1965). The parameter γ_i is the growth efficiency of Z_i.

The term $\varepsilon_i(\sum_{j=1}^{n} Z_j)$ is a closure term (Steele and Henderson, 1981, 1992) that represents predation on the zooplankton by higher trophic levels; since this predation is likely to be generalized rather than specialized, I have assumed that the per-zooplankton predation rate on the ith zooplankton taxon is proportional to total zooplankton biomass $\sum_{j=1}^{n} Z_j$ rather than to the biomass of Z_i alone. Population sizes are measured as their nutrient equivalents, and remineralization of nutrient to its available state is assumed to be instantaneous upon death of individuals, so that the available nutrient N in the system is related to the total concentration T by equation (1c).

One phytoplankton and one zooplankton

Consider first the case with one phytoplankton taxon or size class and one zooplankton taxon or size class ($n = 1$). We can evaluate the stability (the tendency of the system to return to steady state following a perturbation) of this system near its non-trivial equilibrium point (P^*, Z^*) by linearizing equations (1) near that point, yielding the linear approximation:

$$\begin{bmatrix} \frac{dp}{dt} \\ \frac{dz}{dt} \end{bmatrix} = \begin{bmatrix} \frac{\partial f_P}{\partial P} & \frac{\partial f_p}{\partial Z} \\ \frac{\partial f_z}{\partial P} & \frac{\partial f_Z}{\partial Z} \end{bmatrix}_* \begin{bmatrix} p \\ z \end{bmatrix}$$

$$= \begin{bmatrix} P^*\left(\frac{\partial \mu}{\partial N}\frac{\partial N}{\partial P} - Z^*\frac{\partial h}{\partial P}\right) & P^*\left(\frac{\partial \mu}{\partial N}\frac{\partial N}{\partial Z} - h\right) \\ Z^*\frac{\partial(\gamma P h)}{\partial P} & Z^*\frac{\partial \varepsilon}{\partial Z} \end{bmatrix}_* \begin{bmatrix} p \\ z \end{bmatrix} \quad (2)$$

where $p = P - P^*$ and $z = Z - Z^*$ are deviations from steady-state values, and where '*' denotes that all functions and derivatives are evaluated at steady state. Recognizing that $\partial N/\partial P = \partial N/\partial Z = -1$, these equations can be rewritten in terms of the definitions in Table I as:

$$\begin{bmatrix} dp/dt \\ dz/dt \end{bmatrix} = \begin{bmatrix} -a-b & -a-c \\ d & -e \end{bmatrix} \begin{bmatrix} p \\ z \end{bmatrix} \quad (3)$$

The stability of the linearized system can be assessed by finding the eigenvalues λ_i of the matrix of partial derivatives defined above, i.e. by solving for the roots λ_i of the equation $\det A = 0$, where

$$A = \begin{bmatrix} -a-b-\lambda & -a-c \\ d & -e-\lambda \end{bmatrix} \quad (4)$$

Expanding the determinant yields the characteristic equation for this system as

$$\lambda^2 + B_1\lambda + B_2 = 0 \quad (5)$$

where $B_1 = a + b + e$ and $B_2 = e(a + b) + d(a + c)$.

The roots of equation (5) may be calculated using the binomial formula; the system will be locally stable near an equilibrium point (i.e. the system will return to that equilibrium following a small perturbation) if both eigenvalues have negative real parts. Alternatively, Rough–Hurwitz stability criteria (e.g. May 1973) may be used to assess whether all eigenvalues have negative real parts; in particular, a system with two state variables will be locally stable if and only if $B_1 > 0$ and

Table I. Terms (and their signs, when known) for the stability analysis of the model with parallel food chains (Figure 1a). The symbol '$|_*$' denotes that all variables and functions are evaluated at equilibrium.

$a_i = P_i^* \partial \mu_i/\partial N \,|_* > 0$
$b_i = P_i^* Z_i^* \partial h_i/\partial P_i \,|_*$
$c_i = P_i^* h_i \,|_* > 0$
$d_i = Z_i^* \partial(\gamma_i P_i h_i)/\partial P_i \,|_* > 0$
$e_i = Z_i^* \partial \varepsilon_i(\sum_j Z_j)/\partial Z_i \,|_* \geq 0$

$B_2 > 0$. The signs (and possibly magnitudes) of terms $a, \ldots, e$ therefore determine local stability.

Consider first the case where $e = 0$. We expect $a > 0$ since per-capita growth rates increase with nutrient concentration, at least until the concentration becomes toxic. We expect $c > 0$ because P^*h is total per-zooplankton predation rate, which must be positive; and we expect $d > 0$ since the per-zooplankton predation rate (the 'functional response'; Holling, 1965) should increase monotonically with prey density. These three observations show that B_2 is always >0 when $e = 0$.

In contrast, B_1 may be positive or negative, depending on the sign of b, which is determined by the shape of the functional response curve $Ph(P)$. For concave-downwards functional response curves such as the Monod function $P/(P + K_P)$, a line drawn from the origin to any point P on the curve will lie completely under the curve, and the slope of this line at point P will be larger than the slope of the functional response curve itself. Mathematically, at point P we have $h = (Ph)/P > \partial(Ph)/\partial P = h + P\partial h/\partial P$, so that $\partial h(P)/\partial P < 0$; therefore $b < 0$ and will tend to be destabilizing by making B_1 more negative (see Armstrong, 1976). In contrast, S-shaped functional response curves and those with feeding thresholds will have regions where $b > 0$, where they lend a stabilizing influence by making B_1 more positive (Armstrong, 1976; Steele and Henderson, 1992). This tension between the inherently stabilizing property of the phytoplankton response to nutrient concentration and the potentially destabilizing zooplankton functional response to phytoplankton density determines whether the system will be stable or unstable near its non-trivial equilibrium.

We next explore the case $e > 0$, which is taken to represent an increase in predation rates by higher level predators as prey (zooplankton) density increases; Steele and Henderson (1992) advocate Z^{m-1}, $m > 1$, or $Z/(Z + K_Z)$ for the function $\varepsilon(Z)$. From the equations for B_1 and B_2, it is apparent that a system that is stable for $e = 0$ (i.e. has $a + b > 0$) will not be destabilized by $e > 0$, since both B_1 and B_2 will remain >0, while a system that is unstable for $e = 0$ may or may not be stabilized, depending on the magnitude of e [see Steele and Henderson (1992) for further discussion].

n phytoplankton and n zooplankton

Next consider a system composed of n parallel food chains, and assume that they are 'symmetric' in the sense that the growth functions for all taxa at the same trophic level have the same functional forms and the same parameter values (Armstrong, 1982, 1983). Order the equations such that those for successive P_i are odd numbered and those for successive Z_i are even numbered. Then to evaluate the local stability of this system near its non-trivial equilibrium point ($P_1^* = P_2^* = \ldots = P_n^*$, $Z_1^* = Z_2^* = \ldots = Z_n^*$), linearize equations (1) near this point. The linearized system can be written in terms of the definitions in Table I as:

$$\begin{bmatrix} dp_1/dt \\ dz_1/dt \\ dp_2/dt \\ dz_2/dt \\ dp_3/dt \\ dz_3/dt \\ \dots \end{bmatrix} = \begin{bmatrix} -a-b & -a-c & -a & -a & -a & -a & \dots \\ d & -e & 0 & -e & 0 & -e & \dots \\ -a & -a & -a-b & -a-c & -a & -a & \dots \\ 0 & -e & d & -e & 0 & -e & \dots \\ -a & -a & -a & -a & -a-b & -a-c & \dots \\ 0 & -e & 0 & -e & d & -e & \dots \\ \dots & \dots & \dots & \dots & \dots & \dots & \dots \end{bmatrix} \begin{bmatrix} p_1 \\ z_1 \\ p_2 \\ z_2 \\ p_3 \\ z_3 \\ \dots \end{bmatrix} \quad (6)$$

Note that since the system is symmetric, the a_i, b_i, etc., are identical for all i, so that the subscripts can be dropped. Note also that since phytoplankton and zooplankton concentrations are measured as their nutrient equivalents, all the P_i and Z_i affect all the μ_i equally. The stability of the linearized system is found by solving for the eigenvalues λ_i of the $2n \times 2n$ Jacobian matrix defined above, i.e. by solving for the $2n$ roots of the equation:

$$\det \begin{bmatrix} -a-b-\lambda & -a-c & -a & -a & -a & -a & \dots \\ d & -e-\lambda & 0 & -e & 0 & -e & \dots \\ -a & -a & -a-b-\lambda & -a-c & -a & -a & \dots \\ 0 & -e & d & -e-\lambda & 0 & -e & \dots \\ -a & -a & -a & -a & -a-b-\lambda & -a-c & \dots \\ 0 & -e & 0 & -e & d & -e-\lambda & \dots \\ \dots & \dots & \dots & \dots & \dots & \dots & \dots \end{bmatrix} = 0 \quad (7)$$

Elementary row and column manipulations (Lipschutz, 1968) can be used to rewrite equation (7) in a more useful form. First subtract column 1 from columns 3, 5, . . ., $2n-1$ and column 2 from columns 4, 6, . . ., $2n$, producing:

$$\det \begin{bmatrix} -a-b-\lambda & -a-c & b+\lambda & c & b+\lambda & c & \dots \\ d & -e-\lambda & -d & \lambda & -d & \lambda & \dots \\ -a & -a & -b-\lambda & -c & 0 & 0 & \dots \\ 0 & -e & d & -\lambda & 0 & 0 & \dots \\ -a & -a & 0 & 0 & -b-\lambda & -c & \dots \\ 0 & -e & 0 & 0 & d & -\lambda & \dots \\ \dots & \dots & \dots & \dots & \dots & \dots & \dots \end{bmatrix} = 0 \quad (8)$$

[This manipulation makes use of the fact that adding any column in a matrix to any other column, or any row to any other row, does not change the determinant; see, for example, Lipschutz (1968), p. 174.] Then add rows 3, 5, . . ., $2n-1$ to row 1 and rows 4, 6, . . ., $2n$ to row 2 to get:

$$\det \begin{bmatrix} -na-b-\lambda & -na-c & 0 & 0 & 0 & 0 & \dots \\ d & -ne-\lambda & 0 & 0 & 0 & 0 & \dots \\ -a & -a & -b-\lambda & -c & 0 & 0 & \dots \\ 0 & -e & d & -\lambda & 0 & 0 & \dots \\ -a & -a & 0 & 0 & -b-\lambda & -c & \dots \\ 0 & -e & 0 & 0 & d & -\lambda & \dots \\ \dots & \dots & \dots & \dots & \dots & \dots & \dots \end{bmatrix} = 0 \quad (9)$$

Expanding by cofactors the determinant of the 'block-triangular' (Press *et al.*, 1986) matrix (9) yields the characteristic equation:

$$\det A_1 A_2^{n-1} = 0 \tag{10}$$

where

$$A_1 = \begin{bmatrix} -na - b - \lambda & -na - c \\ d & -ne - \lambda \end{bmatrix} \tag{11}$$

and

$$A_2 = \begin{bmatrix} -b - \lambda & -c \\ d & -\lambda \end{bmatrix} \tag{12}$$

Even without solving these equations, it is clear that one pair of eigenvalues (determined from $\det A_1 = 0$) contains all the stabilizing effects of phytoplankton limitation by nutrients (a) and all the potential stabilizing effects of Steele–Henderson predator limitation (e). In contrast, the other $n - 1$ sets of eigenvalues (determined from $\det A_2 = 0$) are bereft of these stabilizing influences and will only be stable if the predator functional response is stabilizing ($b > 0$). It is this reallocation of stabilizing influence among system components that can cause the system to become unstable when multiple food chains are linked through a common nutrient (Armstrong, 1983). The reallocation is from oscillatory modes where phytoplankton densities vary 'out of phase' (where some densities are increasing when others are decreasing) to modes that vary 'in phase' (with all densities changing in parallel). This is apparently what happened in the case of Moloney *et al.* (1991), whose functional response curves are concave downward, and are therefore destabilizing. See the Appendix for further details.

Finally, note that in the symmetric case one could easily stabilize the system with an S-shaped functional response or a feeding threshold; in particular, the feeding thresholds that were used by Armstrong *et al.* (1994) did confer stability to those simulations. However, in systems with non-symmetric parameter values and/or with more complex trophic structures, it is not at all clear that simply adding enough curvature to the functional response curve or adding a feeding threshold, which are used to stabilize within-chain oscillations, will generically stabilize the out-of-phase motions that cause the instability. Instead, a better way to combat instability may be to use a model structure that damps out-of-phase oscillations.

A model of distributed grazing

Consider next a system in which a single state variable G represents the total biomass of zooplankton grazers, and where grazing intensity is distributed among

plankton taxa in proportion to their (past) abundances (Figure 1c). In particular, assume that at steady state a fraction W_i^* of total grazing intensity is directed at taxon i, and that the W_i^* can be calculated as $W_i^* = \psi_i P_i / \sum_j^n \psi_j P_j$ [equation (13c)], where ψ_j is the susceptibility of taxon j to grazing (Armstrong, 1979). This scheme is similar to that used by Fasham *et al*. (1990) to distribute grazing among bacteria, phytoplankton and detritus. An important difference, however, is that here the state variable G is identified not as the abundance of a single species, but as the size of the entire grazing community.

We allow for a lag in the redistribution of grazing intensities as plankton densities change. This lag is embodied in equation (13b), where at any time t the current distribution fractions W_i are assumed to be approaching their steady-state values W_i^* logistically; this mathematical form is appropriate if changes in W_i are driven more by changes in the relative abundances of grazer species than by behavioral changes within prey species (contra the assumption of Fasham *et al*., 1990). Note that away from steady state, the W_i need not sum to unity: far from steady state, the efficiency of the grazing community may be impaired as taxa of grazers that were previously rare increase in response to increases in their prey populations.

The model can be written:

$$\frac{dP_i}{dt} = P_i \left[\mu_i(N) - G\, W_i\, h_i\, (\psi_i\, P_i)\right] \tag{13a}$$

$$\frac{dW_i}{dt} = \alpha_i\, W_i\, (1 - W_i/W_i^*) \tag{13b}$$

$$W_i^* = \psi_i\, P_i / \sum_{j=1}^{n} \psi_j\, P_j \tag{13c}$$

$$\frac{dG}{dt} = G\, [\sum_{i=1}^{n} \gamma_i\, P_i\, W_i\, h_i(\psi_i\, P_i) - \varepsilon(G)] \tag{13d}$$

$$N = T - \sum_{i=1}^{n} P_i - G \tag{13e}$$

Note that the functional response curves h_i are written as functions of susceptibilities ψ_i as well as of densities P_i [equations (13a) and (13d)]; while this notation is of little consequence here, it will facilitate generalizing the model to one that can produce size spectra (see the following section).

In the case with a single phytoplankton taxon, there is no distribution of grazing intensity, so that $W_1 = 1$ and the stability matrix reduces to equation (4). For multiple phytoplankton taxa, put the grazing state variable G in the first row, the P_i in even rows, and the W_i in odd rows starting with row 3. Noting that the P_i^* are all equal, we can then write the stability matrix as:

$$\begin{bmatrix} \mathrm{d}g/\mathrm{d}t \\ \mathrm{d}p_1/\mathrm{d}t \\ \mathrm{d}w_1/\mathrm{d}t \\ \mathrm{d}p_2/\mathrm{d}t \\ \mathrm{d}w_2/\mathrm{d}t \\ \mathrm{d}p_3/\mathrm{d}t \\ \mathrm{d}w_3/\mathrm{d}t \\ \cdots \end{bmatrix} = \begin{bmatrix} -e & d & m & d & m & d & m & \cdots \\ -a-c & -a-b & -f_{ii} & -a & 0 & -a & 0 & \cdots \\ 0 & l_{ii} & -\alpha & l_{ij} & 0 & l_{ij} & 0 & \cdots \\ -a-c & -a & 0 & -a-b & -f_{ii} & -a & 0 & \cdots \\ 0 & l_{ij} & 0 & l_{ij} & -\alpha & l_{ij} & 0 & \cdots \\ -a-c & -a & 0 & -a & 0 & -a-b & -f_{ii} & \cdots \\ 0 & l_{ij} & 0 & l_{ij} & 0 & l_{ii} & -\alpha & \cdots \\ \cdots & \cdots & \cdots & \cdots & \cdots & \cdots & & \cdots \end{bmatrix} \begin{bmatrix} g \\ p_1 \\ w_1 \\ p_2 \\ w_2 \\ p_3 \\ w_3 \\ \cdots \end{bmatrix} \quad (14)$$

The definitions (and signs) of the a_i and c_i (Table II) are unaltered from the model with parallel food webs (Table I). The b_i and d_i are also the same as in Table I, except that the Z_i^* from Table I are replaced by GW_i, and the parameter e is now a function of the single grazing state variable G. The remaining terms correspond straightforwardly.

Application of elementary row and column manipulations to the stability matrix in equation (14) yields the characteristic equation:

$$\det \begin{bmatrix} -e-\lambda & d & m & 0 & 0 & 0 & 0 & \cdots \\ -n(a+c) & -na-b-\lambda & -f_{ii} & 0 & 0 & 0 & 0 & \cdots \\ 0 & l_{ii}+(n-1)l_{ij} & -\alpha-\lambda & 0 & 0 & 0 & 0 & \cdots \\ -a-c & -a & 0 & -b-\lambda & -f_{ii} & 0 & 0 & \cdots \\ 0 & l_{ij} & 0 & l_{ii}-l_{ij} & -\alpha-\lambda & 0 & 0 & \cdots \\ -a-c & -a & 0 & 0 & 0 & -b-\lambda & -f_{ii} & \cdots \\ 0 & l_{ij} & 0 & 0 & 0 & l_{ii}-l_{ij} & -\alpha-\lambda & \cdots \\ \cdots & \cdots & \cdots & \cdots & \cdots & \cdots & \cdots & \cdots \end{bmatrix} = 0 \quad (15)$$

Note that $\partial W_i^*/\partial P_i = (n-1)/(n^2P^*) > 0$ and $\partial W_i^*/\partial P_j = -1/(n^2P^*) < 0$, so that $l_{ii} + (n-1)l_{ij} = 0$. This fact implies that the term in the third row, second column of equation (15) is zero; the eigenvalues are therefore $\lambda = -\alpha$ (once) and the roots of:

$$\det A_3\, A_4^{n-1} = 0 \quad (16)$$

Table II. Terms (and their signs, when known) for the stability analysis of the model with distributed grazing (Figure 1c).

$a_i = P_i^* \partial\mu_i/\partial N\,|_* > 0$
$b_{ii} = P_i^* G^* W_i^* \partial h_i/\partial P_i\,|_*$
$b_{ij} = 0$
$c_i = P_i^* W_i^* h_i\,|_* > 0$
$d_i = G^* \gamma_i W_i^* \partial(P_i h_i)/\partial P_i\,|_* > 0$
$e = G^* \partial\varepsilon(G)/\partial G\,|_* \geq 0$
$f_{ii} = P_i^* G^* h_i\,|_* > 0$
$f_{ij} = 0$
$l_{ii} = \alpha_i \partial W_i^*/\partial P_i\,|_* > 0$
$l_{ij} = \alpha_i \partial W_i^*/\partial P_j\,|_* > 0$
$m_i = G^* \gamma_i P_i^* h_i\,|_* > 0$

where

$$A_3 = \begin{bmatrix} -e - \lambda & d \\ -n(a + c) & -na - b - \lambda \end{bmatrix} \tag{17}$$

and

$$A_4 = \begin{bmatrix} -b - \lambda & -f_{ii} \\ l_{ii} - l_{ij} & -\alpha - \lambda \end{bmatrix} \tag{18}$$

Expanding det $A_3 = 0$ yields the characteristic equation $\lambda^2 + B_1\lambda + B_2 = 0$, where $B_1 = na + b + e$ and $B_2 = e(na + b) + nd(a + c)$. Comparing this result to det $A_1 = 0$ [equation (11)] for parallel food chains, the in-phase modes of both systems will be stable (for $e = 0$) if $na + b > 0$ and will become somewhat more stable for $e > 0$, so that the stability of this mode is comparable in the two models.

However, the out-of-phase modes (whose stability is determined by det $A_4 = 0$) now contain the grazing redistribution rate α on the principal diagonal, so that $B_1 = \alpha + b$ and $B_2 = \alpha b + f_{ii}\,(l_{ii} - l_{ij})$. The first stability condition ($B_1 > 0$) can therefore be satisfied for any b, stabilizing or destabilizing, for α large enough.

The second condition ($B_2 > 0$) requires a bit more work. Using the definitions from Table II, we rewrite B_2 as:

$$\begin{aligned} B_2 &= P^*\, G^*\, \alpha \left[W_i^* \frac{\partial h_i}{\partial P_i} + h_i \left(\frac{\partial W_i^*}{\partial P_i} - \frac{\partial W_i^*}{\partial P_j} \right) \right] \\ &= P^*\, G^*\, \alpha \left[(1/n)\, \partial h_i / \partial P_i + h_i\, (1/nP^*) \right] \end{aligned} \tag{19}$$

The condition $B_2 > 0$ will be satisfied whenever $P_i \partial h_i/\partial P_i + h_i = \partial(P_i h_i)/\partial P_i > 0$; but since $P_i h_i$ is always an increasing function of P_i, $B_2 > 0$ is always satisfied, and the system will be stable whenever $B_1 > 0$ (i.e. whenever $\alpha > \max\{0, -b\}$).

Using the model of distributed grazing to produce plankton size spectra

Plots of abundance within size classes typically show a power-law dependence on size (Sheldon *et al*., 1972; Sprules, 1988; Chisholm, 1992; Gin, 1996; Vidondo *et al*., 1997). However, detailed investigation of these spectra reveals both that they are 'lumpy' (because they represent an idealized fit to the summed abundances of many discrete species; Sprules, 1988) and that they are often not simple power laws (Vidondo *et al*., 1997). Here I show that by allowing for interaction of nearby size classes through common grazers, the model developed in the previous section can produce model size spectra of any general shape. Examination of parameter values in the model may then suggest mechanisms whereby these spectra are created and maintained.

Consider the nutrient density function $n(x)$, where $n(x)\mathrm{d}x$ is the concentration of nutrient between sizes x and $x + \mathrm{d}x$. For convenience, let x be defined as the logarithm of size, $x = \log\,(L/L_0)$, where L is equivalent spherical diameter and L_0

is the (mean) equivalent spherical diameter of some reference size class (Hurtt and Armstrong, 1996, 1999). For a power-law relationship, a plot of $\log(n(x))$ against x will be a straight line.

In reality, the function $n(x)$ is only an idealization of the spectrum produced by the sum of the distributions of several discrete phytoplankton and bacterial populations. To connect this idealized distribution to the underlying distributions of discrete taxa, assume first that individuals of population i are distributed along the size axis according to some function $f_i(x)$, where $\int_{-\infty}^{\infty} f_i(x) = 1$. In this case, the nutrient density of taxon i at size x is the total nutrient concentration in taxon i (P_i) multiplied by $f_i(x)$. Part of the variation in size described by the $f_i(x)$ will be real (e.g. cells in different parts of the cell cycle will have different sizes), part will reflect the range of sizes consumed by a given segment of the grazer spectrum, and part will be due to measurement errors.

Using these functions, we can derive the best least-squares fit of the ensemble of species present to the distribution $n(x)$ by finding values of P_i that minimize the quantity:

$$\int_{-\infty}^{\infty} [n(x) - \sum_i P_i f_i(x)]^2 \, dx \tag{20}$$

This quantity will be minimized when the values of P_i are given by the solutions to the set of linear equations

$$\sum_j C_{ij} P_j = M_i \tag{21}$$

where the quantities

$$C_{ij} \equiv \int f_i(x) f_i(x) \, dx / \int [f_i(x)]^2 \, dx \tag{22a}$$

are normalized commonality coefficients (generalized cosines) between the distributions of i and j, and where the quantities

$$M_i \equiv \int f_i(x) n(x) \, dx / \int [f_i(x)]^2 \, dx \tag{22b}$$

are the normalized number densities of the fitted distribution weighted by the distributions of species i. MacArthur (1970) derived similar equations to describe species competing for food along a size-based resource spectrum. By contrast, in the present model, each species i responds to its own limiting nutrient through its growth rate μ_i, while size-based interaction is through shared grazers.

Equations (21) and the values of the C_{ij} and M_i can now be mapped directly to the terms of the model with distributed grazing. From equation (13a), we have that at steady state:

$$\mu_i = G \, W_i \, h_i \, (\psi_i \, P_i) \tag{23}$$

Using the fact that at steady state $W_i = W_i^*$, and substituting the values of W_i^* from equation (13c), we can rewrite equation (23) as:

$$\mu_i = \kappa\, H_i\,(\psi_i\, P_i) \tag{24}$$

where $H_i(\psi_i P_i) \equiv \psi_i P_i h_i(\psi_i P_i)$ is the total per-grazer grazing rate of grazers associated with species i, and where $\kappa = G/\sum_j \psi_j P_j$ is constant across species.

We can use these observations to link the model of distributed grazing directly to the description of size spectra. First, replace the values of $\psi_i P_i$ in equations (13a) and (13c) with $\sum_j \psi_{ij} C_{ij} P_j$, where ψ_{ij} is the susceptibility of individuals of species j to grazers centered on the distribution of species i. Next, invert equations (24), with the $\psi_i P_i$ replaced by $\sum_j \psi_{ij} C_{ij} P_j$, to obtain:

$$\sum_j \psi_{ij}\, C_{ij}\, P_j = H_i^{-1}(\mu_i/\kappa) \tag{25}$$

Finally, if $\psi_{ij}/\psi_{ii} = 1$ for all i, j, equation (25) becomes exactly equivalent to equation (21), with:

$$M_i \equiv H_i^{-1}(\mu_i/\kappa)/\psi_{ii} \tag{26}$$

so that equation (25) can be used to represent the best least-squares fit to any specified size spectrum $n(x)$. In contrast, if $\psi_{ij} \neq \psi_{ii}$ for some i, j (e.g. if two species are close to the same size, but have different susceptibilities to predation), the fit of the model to any predetermined size spectrum will only be approximate.

These relationships can be used in two ways. First, if we can estimate the functions $f_i(x)$ and the spectrum to be fitted $n(x)$, we can estimate values for the C_{ij} and M_i, then choose values for the growth functions μ_i, the grazing functions H_i, and the susceptibilities ψ_{ii} to yield $M_i = H_i^{-1}(\mu_i/\kappa)/\psi_{ii}$. In this way, the model can be made to reproduce the best steady-state least-squares fit to any desired distribution function $n(x)$. We must assume $\psi_{ij} = \psi_{ii}$ for all i, j to make this procedure work, as noted above.

The second, more scientifically useful application of these results would be to assume growth functions μ_i and predation functions H_i, and to derive the size spectra they imply. For example, consider the form of $\mu_i(x_i)$ under nutrient limitation. Following Aksnes and Egge (1991), Moloney and Field (1991) and Hurtt and Armstrong (1996, 1999), we assume that the half-saturation constants for growth under nutrient limitation $K_{N,i}(x_i)$ are allometric (power-law) functions of x. We also assume that the maximum growth rate is independent of size (Chisholm, 1992). With these assumptions, we can write the following equations for size-dependent growth rates:

$$\mu_i(x_i) = \mu_{\max}\, N/(K_{N,i}(x_i) + N) \tag{27}$$

where

$$\begin{aligned} K_{N,i}(x_i) &= K_N(0)(L_i/L_0)^{\beta_\kappa} \\ &\equiv K_N(0)\, \exp(\beta_K x_i) \end{aligned} \tag{28}$$

and where β_K is the 'allometric coefficient' for growth as a function of nutrient concentration. When $\log(\mu_i(x_i))$ is plotted against x, the resulting curve (Figure

2a) has two straight-line sections connected by a short curved section; the left-hand section has a slope of zero, while the right-hand section has a slope of $-\beta_K$. In Figure 2a, I set $\beta_K = 1$; the 'corner' of the distribution, where $\mu/\mu_{max} = 0.5$, was set at $x = 6$ by choosing $K_N(0)/N$ such that $[K_N(0)/N]\exp(\beta_K x) = 1$ at $x = 6$.

We can use this model of size-dependent growth to generate values for the M_i. In the simplest case where $H_i = aP_i$ and a is a constant, and where $\psi_{ii} = \psi_{ij} \equiv \psi$ for all i and j, we have:

$$M_i(x_i) = \mu_i(x_i)/(a \kappa \psi) \tag{29a}$$

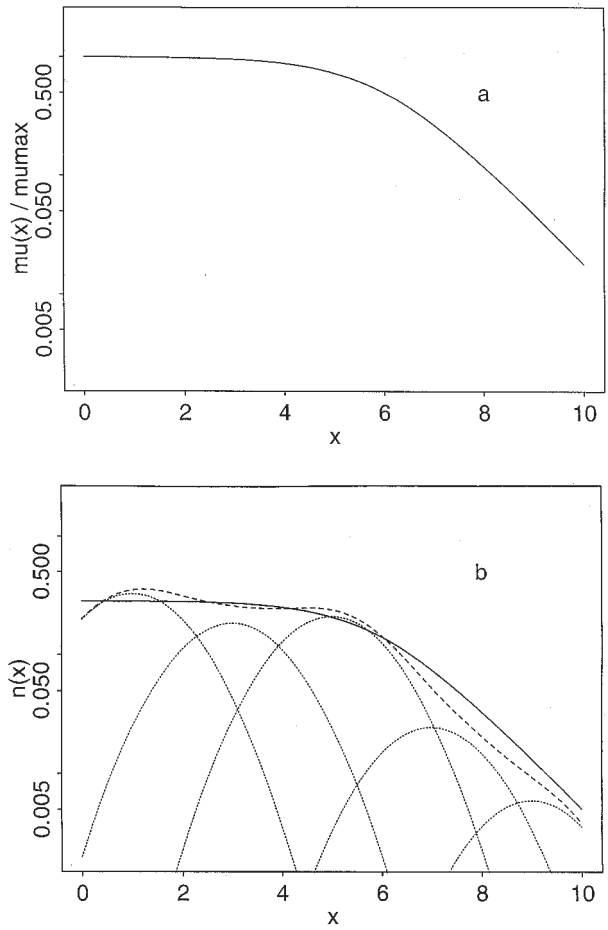

Fig. 2. An example of how the model of distributed grazing can generate size spectra. (**a**) A plot of normalized growth rate μ/μ_{max} versus size x for the model defined by equations (27) and (28). (**b**) A size spectrum of algal abundance generated from the growth rate curve in (a). The dotted lines are the abundances of individual species, the dashed line is the sum of the dotted lines, and the solid line is a reference line that highlights the asymptotic behavior of the summed abundances [equation (31)]. See the text for further explanation.

In this case, the values of M_i are simply proportional to growth rates μ_i.

The C_{ij} are calculated next. In this example, I assume that the $f_i(x)$ are normally distributed with means x_i and variances σ_i^2, so that $f_i(x) = (2\pi\sigma_i^2)^{-1/2} \times \exp\{-(x - x_i)^2/2\sigma_i^2\}$. If we further assume that all the variances are equal, then integrating equation (22a) yields a particularly simple form for the C_{ij}:

$$C_{ij} = \exp\{-(x_i - x_j)^2/4\sigma^2\} \tag{29b}$$

Figure 2b shows the results of combining these assumptions. Calculations were made assuming $\mu_{max}/(a\kappa\psi) = 1$ and $\sigma^2 = 1$. I assumed that five phytoplankton populations were present, with their distributions centered at $x_i = \{1,3,5,7,9\}$. Equations (25) were solved for population sizes P_i, and $P_i f_i(x)$ was plotted for each population (dotted lines). The curve of total nutrient density $\Sigma P_i f_i(x)$ (dashed line) was also plotted.

Qualitatively, the curve of total nutrient density is very similar in shape to the curve for $\mu_i(x_i)$ plotted in Figure 2a; in fact, to the left of the corner, the curve is exactly the pattern of 'equal biomass in equal logarithmic size classes' emphasized by Chisholm (1992). Quantitatively, however, these curves are not the same, since the curve for population size is the best fit to $n(x)$, not to $\mu(x)$, and from equation (22b) it is clear that these two functions are not simply proportional to each other. To see how much they differ, note from equation (22b) that in regions where $n(x)$ is approximately constant:

$$n(x) \approx M_i(x_i) \int [f_i(x)]^2 \, dx / \int f_i(x) \, dx \tag{30}$$

When the $f_i(x)$ are $N(x_i,\sigma^2)$, integrating equation (30) and substituting equation (29a) for the $M_i(x_i)$ yields:

$$n(x) \approx \mu(x) \, (a \, \kappa \, \psi)^{-1} \, (4\pi\sigma^2)^{-1/2} \tag{31}$$

I have plotted equation (31) (with $\sigma^2 = 1$) as the solid line in Figure 2b. Comparison of these two lines shows that on the flat part of the curve, where $\mu(x)$ is approximately constant and equation (31) should apply, the curves for $\Sigma P_i f_i(x)$ and for $n(x)$ are virtually identical; however, on the sloped part of the curves, the curves are offset. Importantly, the comparison also shows that even where there is an offset, the slopes are identical, implying that the asymptotic slope structure is propagated through the integral of equation (22b). This last observation suggests that asymptotic structures created by manipulating the components of equation (25), particularly the functional response curves H_i and the preferences ψ_{ij}, may be useful in suggesting mechanisms for the genesis and maintenance of size spectra, and for representing these structures in models.

Concluding perspective

Trophic relationships in marine food webs are very complicated. In addition to the obvious complications arising from zooplankton life histories with many

stages, there are profound structural switches in marine ecosystems that may promote the functional stability of ecosystems even in the face of oscillations of individual populations (Armstrong, 1982, 1983). When these factors are absent from population models, these models may exhibit extreme instability, and even chaos (Hastings and Powell, 1991). To achieve realistic levels of stability, we must therefore either add these potential stabilizing features or adopt a modeling strategy that produces reliably stable ecosystem functioning without explicit representation of such processes.

Organisms show many behaviors that are potentially stabilizing. First, when conditions become unfavorable, organisms such as diatoms may initiate sexual activity leading to the production of resting stages (Crawford, 1995). By removing these species from the growing part of the phytoplankton community, the production of resting spores should change the dynamics of the interaction of phytoplankton with zooplankton, interrupting the wild swings in the abundances of predators and prey that lead to chaotic behavior. Second, mixotrophy (Sieracki *et al*., 1992), where certain species are autotrophic at some times and heterotrophic at others, could lead to the persistence of these species, with different community roles at different times, in the face of large changes in physical and biotic conditions. Finally, bizarre adaptations, such as the putative killing of diatoms by flagellate bacterivores, leading to enhanced production of bacterial food (Nygaard and Hessen, 1994), may have unknown, but potentially large, effects on the functional stability of marine ecosystems.

It is problematical how long it will be (if ever) before our knowledge of ecosystem structure is complete enough and quantitative enough that we can represent explicitly the feedbacks that may promote functional stability. The empirical study of complex interactions in microbial communities is in its infancy, yet has already shown that ecosystem functions such as community respiration become less variable as biodiversity increases (McGrady-Steed *et al*., 1997). Meanwhile, there is danger that the chaotic behavior of simple food chain models (e.g. Hastings and Powell, 1991) may be taken to represent the aggregate behaviors of autotrophic and heterotrophic parts of the community, through the (incorrect) use of population-level models to represent ecosystem-level processes (Armstrong, 1994).

The distributed grazing model presented above is designed to promote stability of ecosystem functioning without requiring explicit representation of all the processes that could possibly stabilize community function. It is also very flexible. By assigning different maximum growth rates $\mu_{i,max}$, different susceptibilities to grazing ψ_{ij}, and different growth efficiencies γ_i, it should be possible to represent any reasonable set of steady-state phytoplankton densities P_i^*, composite grazer density G^* and free nutrient density N^*. Then, by allowing these quantities to be functions of size, summary curves of species abundance such as in Figure 2b can be raised, lowered, tilted or made more complicated in a variety of ways, allowing the model to reflect the variety of curves obtained in different locations and seasons (Gin, 1996).

The analysis presented in the previous section shows formally how the parameters of the model may be chosen to provide the best least-squares fit to

any specified particle size spectrum, and also gives some indication of how the model may be used to reflect some aspects of mechanism (e.g. size-dependent nutrient uptake). It is less clear how the parameters of the model can be interpreted to represent other aspects of food web structure, such as the interaction of the microbial loop with higher trophic levels (Steele, 1998). However, the fact that the model is capable of representing both aspects of the fundamental duality of plankton community structure, easily reproducing the pattern of 'equal biomass in equal logarithmic size classes' (Chisholm, 1992) while retaining the ability to represent biogeochemical diversity, suggests that finding ways to map other aspects of food web structure onto this model should be a profitable avenue for further investigation.

Acknowledgements

Work with Gail Wolkowicz, Simon Levin and Mercedes Pascual helped greatly in the development of these ideas. I thank Rick Murnane, Jorge Sarmiento and Cindy Lee for helpful comments on the manuscript. The support of NSF grants OCE 93-14707 and OCE 97-12204, NASA grant NAGW-3137, NOAA grant NA56GP0439 and DOE grant DE-FG02-90ER61052 to J.L.Sarmiento is gratefully acknowledged.

References

Aksnes,D.L. and Egge,J.K. (1991) A theoretical model for nutrient uptake in phytoplankton. *Mar. Ecol. Prog. Ser.*, **70**, 65–72.

Armstrong,R.A. (1976) The effects of predator functional response and prey productivity on predator-prey stability: a graphical approach. *Ecology*, **57**, 609–612.

Armstrong,R.A. (1979) Prey species replacement along a gradient of nutrient enrichment: a graphical approach. *Ecology*, **60**, 76–84.

Armstrong,R.A. (1982) The effects of connectivity on community stability. *Am. Nat.*, **120**, 151–170.

Armstrong,R.A. (1983) The role of symmetric food web models in explicating the stability/diversity connection. In DeAngelis,D.L., Post,W.M. and Sugihara,G. (eds), *Current Trends in Food Web Theory.* National Tech. Info. Service, Springfield, VA, pp. 95–99.

Armstrong,R.A. (1994) Grazing limitation and nutrient limitation in marine ecosystems: steady state solutions of an ecosystem model with multiple food chains. *Limnol. Oceanogr.*, **39**, 597–608.

Armstrong,R., Bollens,S., Frost,B., Landry,M., Landsteiner,M. and Moisan,J. (1994) Food webs. In Davis,C.S. and Steele,J.H. (eds), *Biological/Physical Modeling of Upper Ocean Processes. Woods Hole Oceanogr. Inst. Tech. Rep. WHOI-94-32*, Woods Hole, MA, pp. 25–35.

Bissett,W.P., Meyers,M.B., Walsh,J.J. and Muller-Karger,F.E. (1994) The effects of temporal variability of mixed layer depth on primary productivity around Bermuda. *J. Geophys. Res.*, **99(C4)**, 7539–7553.

Broecker,W.S. and Peng,T.-H. (1982) *Tracers in the Sea*. Lamont-Doherty Earth Observatory, Palisades, NY.

Capone,D.G., Zehr,J.P., Paerl,H.W., Bergman,B. and Carpenter,E.J. (1997) *Trichodesmium*, a globally significant marine cyanobacterium. *Science*, **276**, 1221–1229.

Chisholm,S.W. (1992) Phytoplankton size. In Falkowski,P.G. and Woodhead,A.D. (eds), *Primary Productivity and Biogeochemical Cycles in the Sea.* Plenum Press, New York, pp. 213–237.

Crawford,R.M. (1995) The role of sex in the sedimentation of a marine diatom bloom. *Limnol. Oceanogr.*, **40**, 200–204.

Ducklow,H. and Fasham,M.J.R. (1992) Bacteria in the greenhouse: Modeling the role of oceanic plankton in the global carbon cycle. In Mitchell,R. (ed.), *Environmental Microbiology.* Wiley-Liss, New York, NY, pp. 1–31.

Evans,G.R. (1988) A framework for discussing seasonal succession and coexistence of phytoplankton. *Limnol. Oceanogr.*, **14**, 913–920.
Falkowski,P.G. (1997) Evolution of the nitrogen cycle and its influence on the biological sequestration of CO_2 in the ocean. *Nature*, **387**, 272–274.
Fasham,M.J.R., Ducklow,H.W. and McKelvie,S.M. (1990) A nitrogen-based model of plankton dynamics in the oceanic mixed layer. *J. Mar. Res*., **48**, 591–639.
Gin,K.Y.H. (1996) Microbial size spectra from diverse marine ecosystems. PhD Dissertation, MIT/WHOI Joint Program in Ocean Science and Engineering.
Hastings,A. and Powell,T. (1991) Chaos in a three-species food chain. *Ecology*, **73**, 896–903.
Holling,C.S. (1965) The functional response of predators to prey density and its role in mimicry and population regulation. *Mem. Entomol. Soc. Can.,* **45**, 5–60.
Hurtt,G.C. and Armstrong,R.A. (1996) A pelagic ecosystem model calibrated with BATS data. *Deep-Sea Res. II*, **43**, 653–683.
Hurtt,G.C. and Armstrong,R.A. (1999) A pelagic ecosystem model calibrated with BATS and OWS I data. *Deep-Sea Res. I*, **46**, 27–61.
Karl,D., Letelier,R., Tupas,L., Dore,J., Christian,J. and Hebel,D. (1997) The role of nitrogen fixation in biogeochemical cycling in the subtropical North Pacific Ocean. *Nature*, **388**, 533–538.
Lehman,J.T. (1991) Interacting loss and growth rates: the balance of top-down and bottom-up controls in plankton communities. *Limnol. Oceanogr.*, **36**, 1546–1554.
Letelier,R.M., Bidigare,R.R., Hebel,D.V., Ondrusek,M., Winn,C.D. and Karl,D.M. (1993) Temporal variability of phytoplankton community structure based on pigment analysis. *Limnol. Oceanogr.*, **38**, 1420–1437.
Lipschutz,S. (1968) *Linear Algebra*. McGraw-Hill, New York, NY.
MacArthur,R.H. (1970) Species packing and competitive equilibrium among many species. *Theor. Popul. Biol*., **1**, 1–11.
Maier-Reimer,E. (1993) Geochemical cycles in an ocean general circulation model. Preindustrial tracer distributions. *Global Biogeochem. Cycles*, **7**, 645–677.
May,R.M. (1973) *Stability and Complexity in Model Ecosystems*. Princeton University Press, Princeton, NJ.
McGrady-Steed,J., Harris,P.M. and Morin,P.J. (1997) Biodiversity regulates ecosystem stability. *Nature*, **390**, 162–165.
Moloney,C.L. and Field,J.G. (1989) General allometric equations for rates of nutrient uptake, ingestion and respiration in plankton organisms. *Limnol. Oceanogr.*, **34**, 1290–1299.
Moloney,C.L. and Field,J.G. (1991) The size-based dynamics of plankton food webs. I. A simulation model of carbon and nitrogen flows. *J. Plankton Res.*, **13**, 1003–1038.
Moloney,C.L., Field,J.G. and Lucas,M.I. (1991) The size-based dynamics of plankton food webs. II. Simulations of three contrasting Benguela food webs. *J. Plankton Res.*, **13**, 1039–1092.
Nygaard,K. and Hessen,D.O. (1994) Diatom kills by flagellates. *Nature*, **367**, 520.
Press,W.H., Flannery,B.P., Teukolsky,S.A. and Vetterling,W.T. (1986) *Numerical Recipes*. Cambridge University Press, New York, NY.
Raimbault,P., Rodier,M. and Taupier-Letage,I. (1988) Size fraction of phytoplankton in the Ligurian Sea and the Algerian Basin (Mediterranean Sea): size distribution versus total concentration. *Mar. Microb. Food Webs*, **3**, 1–7.
Sheldon,R.W., Prakash,A. and Sutcliffe,W.H. (1972) The size distribution of particles in the ocean. *Limnol. Oceanogr.*, **17**, 327–339.
Sieracki,M.E., Verity,P.G. and Stoecker,D.K. (1992) Plankton community response to sequential silicate and nitrate depletion during the 1989 North Atlantic spring bloom. *Deep-Sea Res. II*, **40**, 213–225.
Sprules,W.G. (1988) Effects of trophic interactions on the shape of pelagic size spectra. *Verh. Int. Ver. Limnol*., **23**, 234–240.
Steele,J.H. (1998) Incorporating the microbial loop in a simple plankton model. *Proc. R. Soc. London Ser. B*, **265**, 1771–1777.
Steele,J.H and Henderson,E. (1981) A simple plankton model. *Am. Nat.*, **117**, 676–691.
Steele,J.H and Henderson,E. (1992) The role of predation in plankton models. *J. Plankton Res.*, **14**, 157–172.
Taylor,A.H. and Joint,I. (1990) A steady-state analysis of the 'microbial loop' in stratified systems. *Mar. Ecol. Prog. Ser.*, **59**, 1–17.
Thingstad,T.F. and Sakshaug,E. (1990) Control of phytoplankton growth in nutrient recycling systems. *Mar. Ecol. Prog. Ser.*, **63**, 261–272.

Totterdell,I., Armstrong,R.A., Drange,H., Parslow,J.S., Powell,T.M. and Taylor,A.H. (1993) Trophic resolution. In Evans,G.T. and Fasham,M.J.R. (eds), *Towards a Model of Ocean Biogeochemical Processes.* Springer-Verlag, New York, NY, pp. 71–92.

Vidondo,B., Prairie,Y.T., Blanco,J.M. and Duarte,C.M. (1997) Some aspects of the analysis of size spectra in aquatic ecology. *Limnol. Oceanogr.*, **42**, 184–192.

Received on December 16, 1997; accepted on October 14, 1998

Appendix

In the model with multiple parallel food chains, the eigenvalues λ_i from matrix A_1 [equation (11)] have eigenvectors $\xi_i{}^T = (\xi_{i1}, \xi_{i2}, \ldots)$ in which $\xi_{i1} = \xi_{i3} = \xi_{i5} = \ldots$, corresponding to motions in which the densities of all phytoplankton taxa rise or fall together ('in phase'). In these eigenvectors, it is also true that $\xi_{i2} = \xi_{i4} = \xi_{i6} = \ldots$, so that zooplankton densities also rise or fall in phase with one another (though out of phase with the phytoplankton taxa). In contrast, the other sets of eigenvalues [from matrix A_2, equation (12)] do not have this structure, so that individual phytoplankton (zooplankton) taxa may oscillate 'out of phase' (i.e. some can be increasing while others are decreasing).

To see this, we must assess the structure of the eigenvectors of the linearized matrix [call it M: equation (6)]. In particular, we must determine for which eigenvalues λ_i the associated eigenvectors ξ_i are structured such that odd-numbered elements (ξ_{i1}, ξ_{i3}, ξ_{i5}, ...) are all equal and even-numbered elements (ξ_{i2}, ξ_{i4}, ξ_{i6}, ...) are also all equal, and which eigenvalues do not have this structure. Since the model is symmetric (though the matrix M is not), it will suffice to ascertain the relationship between the first pair of eigenvector elements (ξ_{i1}, ξ_{i2}) and any other pair ($\xi_{i,2j+1}, \xi_{i,2j+2}$), $j \geq 1$; without loss of generality we choose $j = 1$. For the ith eigenvalue λ_i, we write the first four terms of $[M - \lambda_i I]$ $\xi_i = 0$ as:

$$\begin{array}{rrrrl} -(a+b+\lambda_i)\xi_{i1} & -(a+c)\xi_{i2} & -a\xi_{i3} & -a\xi_{i4} & + \ \ldots = 0 \\ d\xi_{i1} & -(e+\lambda_i)\xi_{i2} & & -e\xi_{i4} & + \ \ldots = 0 \\ -a\xi_{i1} & -a\xi_{i2} & -(a+b+\lambda_i)\xi_{i3} & -(a+c)\xi_{i4} & + \ \ldots = 0 \\ & -e\xi_{i2} & d\xi_{i3} & -(e+\lambda_i)\xi_{i4} & + \ \ldots = 0 \end{array} \qquad \text{(A1)}$$

Subtracting the third equation from the first and the fourth from the second yields:

$$\begin{array}{rr} -(b+\lambda_i)\,(\xi_{i1} - \xi_{i3}) & -c\,(\xi_{i2} - \xi_{i4}) = 0 \\ -d\,(\xi_{i1} - \xi_{i3}) & -\lambda_i\,(\xi_{i2} - \xi_{i4}) = 0 \end{array} \qquad \text{(A2)}$$

(Note that the terms '. . .' in these four equations vanish.) We then rewrite these equations in matrix form as:

$$\begin{bmatrix} -b-\lambda_i & -c \\ d & -\lambda_i \end{bmatrix} \begin{bmatrix} \xi_{i1} - \xi_{i3} \\ \xi_{i2} - \xi_{i14} \end{bmatrix} = 0 \qquad \text{(A3)}$$

Note that the matrix in equation (A3) is identical to A_2 [equation (12)]. Therefore, when λ_i is a root of matrix A_2, the determinant of the matrix in equation ($A3$) is 0 and eigenvectors with $\xi_{i1} \neq \xi_{i3}$ and $\xi_{i2} \neq \xi_{i4}$ exist. In contrast, for all other values of λ_i [e.g. the roots of matrix A_1, equation (11)], the determinant of matrix equation (A3) is not zero, and the only solution is $\xi_{i1} - \xi_{i3} = 0$ and $\xi_{i2} - \xi_{i4} = 0$, so that all phytoplankton densities must vary 'in phase' with one another. Similar arguments apply to the models with distributed grazing.